POLITECNICO DI TORINO
Repository ISTITUZIONALE

An axiomatic/asymptotic evaluation of best theories for isotropic metallic and functionally graded plates employing non-polynomic functions

(Article begins on next page)

30 January 2025

Accepted Manuscript

An axiomatic/asymptotic evaluation of best theories for isotropic metallic and functionally graded plates employing non-polynomic functions

S. Candiotti, J.L. Mantari, J. Yarasca, M. Petrolo, E. Carrera

Please cite this article in press as: S. Candiotti et al., An axiomatic/asymptotic evaluation of best theories for isotropic metallic and functionally graded plates employing non-polynomic functions, *Aerosp. Sci. Technol.* (2017), http://dx.doi.org/10.1016/j.ast.2017.05.003

An axiomatic/asymptotic evaluation of best theories for isotropic metallic and functionally graded plates employing non-polynomic functions

S. Candiotti [a], J. L. Mantari [a,b,1], J. Yarasca [a], M. Petrolo [c], E. Carrera [c]

[a] *Faculty of Mechanical Engineering, Universidad de Ingeniería y Tecnología (UTEC), Medrano Silva 165, Barranco, Lima, Perú*

[b] *University of New Mexico, Department of Mechanical Engineering, Albuquerque, New Mexico, U.S.A.*

[c] *MUL² Team, Department of Mechanical and Aerospace Engineering, Politecnico di Torino, Corso Duca degli Abruzzi 24, 10129, Torino, Italy*

---

[1]Corresponding Author email: jmantari@utec.edu.pe Tel: +00511 3540070; Cell: +0051 962224551;

** This manuscript has not been published elsewhere and that it has not been submitted simultaneously for publication elsewhere.

An axiomatic/asymptotic evaluation of best theories for isotropic metallic and functionally graded plates employing non-polynomic functions

This paper presents Best Theory Diagrams (BTDs) constructed from various non-polynomial terms to identify best plate theories for metallic and functionally graded plates. The BTD is a curve that provides the minimum number of unknown variables necessary to obtain a given accuracy or the best accuracy given by a given number of unknown variables. The plate theories that belong to the BTD have been obtained using the Axiomatic/Asymptotic Method (AAM). The different plate theories reported are implemented by using the Carrera Unified Formulation (CUF). Navier-type solutions have been obtained for the case of simply supported plates loaded by a bisinuisoidal transverse pressure with different length-to-thickness ratios. The BTDs built from non-polynomial functions are compared with BTDs using Maclaurin expansions. The results suggest that the plate models obtained from the BTD using non-polynomial terms can improve the accuracy obtained from Maclaurin expansions for a given number of unknown variables of the displacement field.

1. Introduction

The development of plate models for isotropic, laminated and functionally graded plates with lower computational costs while retaining accurate results represents one of the most important issues of structural analysis. The most accurate results are obtained by employing the 3D elasticity equations at the expense of high computational cost. This 3D deformation state can be simplified using axiomatic hypotheses based on conjectures and experience. Under these hypotheses, the simplest plate theory include the classical plate theories (CLP)

developed by Kirchhoff-Love [1-2] which is only suitable for thin plates cases when the shear effect can be neglected. To analyze shear stress and thick plates, the First-order Shear Deformation Theories (FSDT) were developed originally by Reissner [3] and Mindlin[4]. In order to study structural problems of higher complexity where CLP and FSDT fail to give accurate results, the Higher order Shear Deformation Theories (HSDT) were proposed. The HSDT have the advantage of being able to be developed by expanding the displacement components in polynomial and non-polynomial series of the thickness coordinate for any desired order, improving the accuracy in exchange for computational cost. One of the best known models of HSTD include the work of Reddy [5], better know as the Third order Shear Deformation Theory (TSDT) which was extended for the analysis of termomechanical functionally graded plates (FGP) in Ref. [6].

The present paper is embedded in the framework of the Carrera Unified Formulation (CUF) [8] which can be seen as a unified approach to building any order structural model. In fact, the CUF makes it possible for plate analysis to define the displacement and stress fields as the arbitrary expansion of the thickness coordinate of any desired order. The equilibrium equations can be written according to few fundamental nuclei whose form does not depend on either the expansion order or on the choices made for the base functions. More comprehensive CUF literature overviews can be found in Refs. [9-11].

Additionally the CUF has been extended to the study of functionally graded plates by Brischetto and Carrera [12-18], including cases of thermo-mechanical bending, refined models for piezoelectric plates and the effects of thickness stretching.

In order to reduce the computational cost, the Axiomatic/Asymptotic Method (AAM), introduced by Carrera and Petrolo [19-34], can provide asymptotic-like results starting from a preliminary axiomatic theory by evaluating the effectiveness of each term against a reference solution and retaining those variables whose influence cannot be neglected. The BTD is stemmed from the AAM [21] as a tool to evaluate the best models against given accuracies or computational costs.

This paper uses non-polynomial models to build refined plate theories. The use of non-polynomial models has been studied previously in many works. Levy [35] was the first to

develop a displacement field based on the sinusoidal function for an isotropic elastic plate. Stein [36] developed refined plate theories expressing the displacement field with trigonometric functions to represent the thickness effect and approximated the shear stress distribution through the thickness. The sinusoidal shear deformation theory was presented by Touratier [37] as an effective alternative to the FSDT without requiring shear correction factors. Karama et al. [38] introduced an exponential function as a shear stress function and found it to be richer than a sine function. Shimpi and Ghugal [39] used a layerwise trigonometric shear deformation theory for the study of two layered cross-ply laminated beams. A zig-zag model for laminated composite beams with a trigonometric displacement field across the thickness was proposed by Arya et al. [40] and was extended for symmetric composite plates by Ferreira et al. [41] giving better results than FSDT. Neves et al. [42-45] developed multiple trigonometric and hyperbolic shear deformation theories for the static and dynamic analysis of functionally graded plates. A new trigonometric shear deformation theory for isotropic, laminated composite and sandwich plates was developed by Mantari et al. [46]. Tounsi et al [47] presented a refined trigonometric shear deformation theory for thermoelastic bending of functionally graded sandwich plates with only four functions variables. Sahoo et al [48] proposed a new trigonometric zigzag theory for static analysis of laminated composite and sandwich plates based upon the secant function. Mantari et al. [49] and Ramos et al. [50] proposed new non-polynomial displacement field expansions and showed how to improve results by optimization of those functions. Results and discussion of hybrid functions have been presented by Filippi et al. [51, 52] showing that the linear contribution to trigonometric series leads to the reduction of trigonometric terms required to reach the reference solutions. A simply four unknows refied theory was presented by Zenkour [61-63] for the analysis of bending in functionally graded plates, and later was used in the static, dynamic and buckling analysis of functionally graded isotropic and sandwich plates by Thai et al [64]. The general recommendations to develop 4 unknows quasi-3D HSDTs to study functionally graded plates were discussed by Mantari [53] consisting in the proper selection of parameters in several non-polynomial theories.

In this paper, the CUF is used to obtain reduced models with non-polynomial functions used as displacement field for isotropic aluminum, bimetallic and functionally graded plates of various thickness ratios. Best plate theory diagrams are obtained for each proposed non-

polynomial model and afterward are compared against the Maclaurin expansion BTDs. This paper is organized as follows: a brief description of the CUF formulation is given in Section 2; the asymptotic-axiomatic method is presented in Section 3, while results are discussed in Section 4. Finally, conclusions are given in Section 5.

2. Refined theories based on Carrera Unified Formulation

Plate geometry and notations are given in Fig. 1. According to Carrera [8], the displacement of a plate model is given by

$$\mathbf{u}(x, y, z) = F_\tau(z). u_\tau(x, y) \qquad \tau = 0, 1, 2, ..., N$$

$$\boldsymbol{\delta u}(x, y, z) = F_s(z). \delta u_s(x, y) \qquad s = 0, 1, 2, ..., N \qquad (1a\text{-}b)$$

where $\mathbf{u}$ is the displacement vector (u_x, u_y, u_z) and N is the number of terms of the expansion. The expansion functions F_τ and F_s can be defined on the overall thickness of the plate. According to Einstein's notation, the repeated subscript τ and s indicates summation. In this paper, the Equivalent Single Layer (ESL) scheme was used. An example of a displacement field using a fourth order Maclaurin expansion (ED4) is presented below:

$$u_x = u_{x0} + z u_{x1} + z^2 u_{x2} + z^3 u_{x3} + z^4 u_{x4}$$

$$u_y = u_{y0} + z u_{y1} + z^2 u_{y2} + z^3 u_{y3} + z^4 u_{y4}$$

$$u_z = u_{z0} + z u_{z1} + z^2 u_{z2} + z^3 u_{z3} + z^4 u_{z4} \qquad (2a\text{-}c)$$

ESL models based on Maclaurin expansions are indicated as EDN where N is the order of the expansion.

In addition to the polynomial expansion (*pol*), this paper uses functions presented by Mantari et al. [49]: a sine-cosine expansion (*sin*), an hyperbolic expansion (*hyp*), and a new exponential expansion (*exp)*, see Table 1.

2.1. Elastic stress–strain relation

The stress (σ) and the strain (ε) are grouped as follows:

$$\boldsymbol{\sigma}_p^k = \begin{bmatrix} \sigma_{xx}^k & \sigma_{yy}^k & \sigma_{xy}^k \end{bmatrix}^T, \qquad \boldsymbol{\sigma}_n^k = \begin{bmatrix} \sigma_{xz}^k & \sigma_{yz}^k & \sigma_{zz}^k \end{bmatrix}^T,$$

$$\boldsymbol{\varepsilon}_p^k = \begin{bmatrix} \varepsilon_{xx}^k & \varepsilon_{yy}^k & \gamma_{xy}^k \end{bmatrix}^T, \qquad \boldsymbol{\varepsilon}_n^k = \begin{bmatrix} \gamma_{xz}^k & \gamma_{yz}^k & \varepsilon_{zz}^k \end{bmatrix}^T, \tag{3a-d}$$

The subscript "p" is related to the in-plane components, while "n" to the out-of-plane components, the strain – displacement relationships are given as:

$$\boldsymbol{\varepsilon}_p^k = D_p \mathbf{u}^k,$$

$$\boldsymbol{\varepsilon}_n^k = D_n \mathbf{u}^k = \left(D_{np} + D_{nz} \right) \mathbf{u}^k,$$

$$D_p = \begin{bmatrix} \frac{\partial}{\partial x} & 0 & 0 \\ 0 & \frac{\partial}{\partial y} & 0 \\ \frac{\partial}{\partial y} & \frac{\partial}{\partial x} & 0 \end{bmatrix}, \quad D_{np} = \begin{bmatrix} 0 & 0 & \frac{\partial}{\partial x} \\ 0 & 0 & \frac{\partial}{\partial y} \\ 0 & 0 & 0 \end{bmatrix}, \quad D_{nz} = \begin{bmatrix} \frac{\partial}{\partial z} & 0 & 0 \\ 0 & \frac{\partial}{\partial z} & 0 \\ 0 & 0 & \frac{\partial}{\partial z} \end{bmatrix} \tag{4a-e}$$

The stress – strain relationships corresponding to an isotropic material can be expressed according to the Hooke law:

$$\boldsymbol{\sigma}^k = C^k \boldsymbol{\varepsilon}^k,$$

$$\begin{Bmatrix} \sigma_{xx}^k \\ \sigma_{yy}^k \\ \sigma_{xy}^k \\ \sigma_{yz}^k \\ \sigma_{xz}^k \\ \sigma_{zz}^k \end{Bmatrix} = \begin{bmatrix} C_{11}^k & C_{12}^k & 0 & 0 & 0 & C_{13}^k \\ C_{12}^k & C_{22}^k & 0 & 0 & 0 & C_{23}^k \\ 0 & 0 & C_{66}^k & 0 & 0 & 0 \\ 0 & 0 & 0 & C_{44}^k & 0 & 0 \\ 0 & 0 & 0 & 0 & C_{55}^k & 0 \\ C_{13}^k & C_{23}^k & 0 & 0 & 0 & C_{33}^k \end{bmatrix} \begin{Bmatrix} \varepsilon_{xx}^k \\ \varepsilon_{yy}^k \\ \gamma_{xy}^k \\ \gamma_{yz}^k \\ \gamma_{xz}^k \\ \varepsilon_{zz}^k \end{Bmatrix} \tag{5a-b}$$

and the stiffness coefficients C_{ij} in terms of the engineering constants are

$$C_{11}^k = C_{22}^k = C_{33}^k = \frac{(1 - v^k)E(z)^k}{(1 + v^k)(1 - 2v^k)}$$

$$C_{12}^k = C_{13}^k = C_{23}^k = \frac{v^k E(z)^k}{(1 + v^k)(1 - 2v^k)}$$

$$C_{44}^k = C_{55}^k = C_{66}^k = \frac{E(z)^k}{2(1+v^k)} \tag{6a-c}$$

In the metallic and bimetallic case, the Young and shear modulus are considered constant, while in the case of functionally graded plates, the material properties can vary through the thickness with a power law distribution, which is presented as follows:

$$P(z) = (P_t - P_b)V_c(z) + P_b$$

$$V_c(z) = \left(\frac{2z+h}{2h}\right)^p, \quad -\frac{h}{2} \leq z \leq \frac{h}{2} \tag{7a-b}$$

Where $P(z)$ stand for a material propertie, P_t and P_b are the material propertie of the top and bottom faces of the plate, and p is the exponent that specifies the material propertie variation through the thickness. The properties affected by the power law are the Young modulus and the shear modulus. The poisson ratio is considered constant through all the paper.

Afterwards, the stiffness coefficients can be grouped as follows:

$$C_{pp}^k = \begin{bmatrix} C_{11}^k & C_{12}^k & 0 \\ C_{12}^k & C_{22}^k & 0 \\ 0 & 0 & C_{66}^k \end{bmatrix} \quad C_{pn}^k = \begin{bmatrix} 0 & 0 & C_{13}^k \\ 0 & 0 & C_{23}^k \\ 0 & 0 & 0 \end{bmatrix}$$

$$C_{np}^k = \begin{bmatrix} 0 & 0 & 0 \\ 0 & 0 & 0 \\ C_{13}^k & C_{23}^k & 0 \end{bmatrix} \quad C_{nn}^k = \begin{bmatrix} C_{55}^k & 0 & 0 \\ 0 & C_{44}^k & 0 \\ 0 & 0 & C_{33}^k \end{bmatrix} \tag{8a-d}$$

The Hooke law can be defined regarding the in-plane and out-of-plane terms:

$$\sigma_p^k = \left(C_{pp}\varepsilon_p^k + C_{pn}\varepsilon_n^k\right),$$

$$\sigma_n^k = \left(C_{np}\varepsilon_p^k + C_{nn}\varepsilon_n^k\right) \tag{9a-b}$$

2.2. Governing Equations

The plate static analysis considers the equilibrium via the principle of virtual displacement (PVD) as follows:

$$\delta L_{int} = \delta L_{ext} \tag{10}$$

where δL_{int} is the virtual variation of the internal work and δL_{ext} is the virtual variation of the external work. The PVD can be written as:

$$\sum_{k=1}^{N_l} \int_z \int_\Omega \left(\delta \boldsymbol{\varepsilon}_p^{k^T} \boldsymbol{\sigma}_p^k + \delta \boldsymbol{\varepsilon}_n^{k^T} \boldsymbol{\sigma}_n^k \right) d\Omega dz = \sum_{k=1}^{N_l} \delta L_{ext}^k \tag{11}$$

Further details on the application of PVD to plates can be found in Refs. [9, 10]. The final result is two systems of differential equations:

The governing equations are:

$$\mathbf{K}_d^{k\tau s} \mathbf{u}_\tau^k = \mathbf{p}_s^k \tag{12}$$

With boundary condition stated as:

$$\mathbf{\Pi}_d^{k\tau s} \mathbf{u}_\tau = \mathbf{\Pi}_d^{k\tau s} \overline{\mathbf{u}}_\tau \tag{13}$$

$\mathbf{p}_\tau$ is the external load. The fundamental nucleus, $\mathbf{K}_d^{\tau s}$, is assembled trough the indexes, τ and s considering the order of expansion in z for the displacement field.

2.3. Analytical solution

Navier-type closed-form solutions have been obtained for the case of simply supported plates. The displacement variable and the transversely distributed load can be expressed in the following Fourier series:

$$u_{x\tau} = \sum_{m,n} (U_{x\tau}) \cos(\alpha x) \sin(\beta y) \qquad\qquad 0 \leq x \leq a; \ 0 \leq y \leq b$$

$$u_{y\tau} = \sum_{m,n} (U_{y\tau}) \sin(\alpha x) \cos(\beta y) \qquad\qquad 0 \leq x \leq a; 0 \leq y \leq b$$

$$u_{z\tau} = \sum_{m,n} (U_{z\tau}) \sin(\alpha x) \sin(\beta y) \qquad\qquad 0 \leq x \leq a; 0 \leq y \leq b$$

$$p_z = \sum_{m,n} (P_z) \sin(\alpha x) \sin(\beta y) \qquad\qquad 0 \leq x \leq a; 0 \leq y \leq b$$

$$\alpha = \frac{m\pi}{a}, \qquad \beta = \frac{n\pi}{b} \tag{14a-f}$$

where $U_{x\tau}^k, U_{y\tau}^k, U_{z\tau}^k$ and Q_z are the amplitudes, m and n are the number of waves (which can range from 0 to ∞) and a and b are the plate lengths in the x and y direction respectively.

Applying Eq. (14a-f), the governing equation (12) becomes:

$$\begin{bmatrix} K_{11} & K_{12} & K_{13} \\ K_{21} & K_{22} & K_{23} \\ K_{31} & K_{32} & K_{33} \end{bmatrix} \begin{bmatrix} U_{xt} \\ U_{yt} \\ U_{zt} \end{bmatrix} = \begin{bmatrix} 0 \\ 0 \\ F_s P_z \end{bmatrix} \tag{15}$$

Where:

$$K_{11} = \int_z \left(C_{55} F_{\tau,z} F_{s,z} + \alpha^2 C_{11} F_\tau F_s + \beta^2 C_{66} F_\tau F_s \right) dz$$

$$K_{12} = \int_z (\alpha\beta C_{12} F_\tau F_s + \alpha\beta C_{66} F_\tau F_s) dz$$

$$K_{13} = \int_z \left(-\alpha C_{13} F_\tau F_{s,z} + \alpha C_{55} F_{\tau,z} F_s \right) dz$$

$$K_{21} = \int_z (\alpha\beta C_{12} F_\tau F_s + \alpha\beta C_{66} F_\tau F_s) dz$$

$$K_{22} = \int_z \left(C_{44} F_{\tau,z} F_{s,z} + \alpha^2 C_{66} F_\tau F_s + \beta^2 C_{22} F_\tau F_s \right) dz$$

$$K_{23} = \int_z \left(-\beta C_{23} F_\tau F_{s,z} + \beta C_{44} F_{\tau,z} F_s \right) dz$$

$$K_{31} = \int_z \left(\alpha C_{55} F_\tau F_{s,z} - \alpha C_{13} F_{\tau,z} F_s \right) dz$$

$$K_{32} = \int_z \left(\beta C_{44} F_\tau F_{s,z} - \beta C_{23} F_{\tau,z} F_s \right) dz$$

$$K_{33} = \int_z \left(C_{33} F_{\tau,z} F_{s,z} + \alpha^2 C_{55} F_\tau F_s + \beta^2 C_{44} F_\tau F_s \right) dz \tag{16a-i}$$

3. Axiomatic/Asymptotic Method and the Best Theory Diagram

Refined plate theories offer significant advantages regarding the accuracy of the solution and detection of non-classical effects. The drawback of these theories is that a higher computational cost is incurred because of the presence of a large number of displacement variables. Previous works [19, 20] have highlighted that the terms of the expansion do not

have the same influence and it is possible to obtain reduced models which show the same accuracy as the full model. As reported in [19] the effectiveness of each term can be investigated as follows:

1. The problem data are fixed (i.e. geometry, boundary conditions, loadings, materials).

2. A set of output variables is chosen (e.g. maximum displacement, stress/displacement component at a given point).

3. The CUF is used to generate the governing equations for the considered theories.

4. A reference solution is used to establish the accuracy (in this paper a full LD4 theory is used as best – reference results).

5. A theory is chosen, that is, the terms that have to be considered in the expansion of u_x, u_y and u_z are established.

6. The accuracy of each model is numerically established by measuring the error produced.

7. The most suitable kinematic model for a given structural problem is then obtained by discarding the noneffective displacement variables.

A graphic notation is introduced to improve the readability of the results. This consists of a table with three rows, and a number of columns equal to the number of the displacement variable used in the expansion. An example is given to explain how the evaluation of the effectiveness of the displacement variables is carried out by deactivating u_{x1} in a fourth order model is presented in Table 2. The notation adopted for active and inactive terms is given in Table 3.

The BTD can be built by evaluating the accuracy of all the models given by combining all the terms of an expansion. Therefore, for each expansion of this paper, 2^{15} models were evaluated. The BTD is made of all those models that, for a given accuracy, require the least number of terms. Or, conversely, for a given number of terms, the BTD model provides the best accuracy.

4. Results and discussions

The results deal with aluminum, bimetallic and functional graduated simply supported square plates. The load is a bisinusoidal transverse pressure applied at the top surface of the plate,

$$p = \bar{p}_z \cdot \sin\left(\frac{m\pi x}{a}\right) \sin\left(\frac{n\pi y}{b}\right) \tag{17}$$

In all analyses, $\bar{p}_z$ is equal to 1 kPa, and the number of waves m and n are equal to $m = n = 1$. Geometrical notations and reference system are given in Fig. 1.

Reduced models are developed to evaluate normal stress $\bar{\sigma}_{xx}$ for the aluminum plate, and $\bar{\sigma}_{xx}$ and $\bar{\sigma}_{xz}$ in the case of the bimetallic and functionally graded plate. The results are computed at $(\frac{a}{2}, \frac{b}{2}, z)$ with $-\frac{h}{2} \leq z \leq \frac{h}{2}$, where h is the total thickness of the plate, as in [54, 55]. Shear stresses are evaluated through the integration of the equilibrium equations. The following expressions normalize stresses for the different analysis:

Aluminum and bimetallic plates

$$\bar{\sigma}_{xx} = \sigma_{xx}\left(\frac{h^2}{a^2 \bar{p}_z}\right);$$

$$\bar{\sigma}_{xz} = \sigma_{xz}\left(\frac{h}{a \bar{p}_z}\right); \tag{18a-b}$$

Functionally graded plate

$$\bar{\sigma}_{xx} = \sigma_{xx}\left(\frac{h}{a \bar{p}_z}\right);$$

$$\bar{\sigma}_{xz} = \sigma_{xz}\left(\frac{h}{a \bar{p}_z}\right); \tag{19a-b}$$

Higher order models from the open literature are used for comparison purposes. These model are obtained by using the CUF and are presented as follows:

FSDT (Ref [3-4])

$$u_x = u_{x0} + z u_{x1}$$

$$u_y = u_{y0} + z u_{y1}$$

$$u_z = u_{z0} \qquad\qquad (20a\text{-}c)$$

Pandya (Ref [57])

$$u_x = u_{x0} + z u_{x1} + z^2 u_{x2} + z^3 u_{x3}$$

$$u_y = u_{y0} + z u_{y1} + z^2 u_{y2} + z^3 u_{y3}$$

$$u_z = u_{z0} \qquad\qquad (21a\text{-}c)$$

Roque (Ref [58])

$$u_x = u_{x0} + z u_{x1} + z^3 u_{x3}$$

$$u_y = u_{y0} + z u_{y1} + z^3 u_{y3}$$

$$u_z = u_{z0} \qquad\qquad (22a\text{-}c)$$

Kant (Ref [59])

$$u_x = u_{x0} + z u_{x1} + z^2 u_{x2} + z^3 u_{x3}$$

$$u_y = u_{y0} + z u_{y1} + z^2 u_{y2} + z^3 u_{y3}$$

$$u_z = u_{z0} + z u_{z1} + z^2 u_{z2} + z^3 u_{z3} \qquad\qquad (23a\text{-}c)$$

Lo (Ref [60])

$$u_x = u_{x0} + z u_{x1} + z^2 u_{x2} + z^3 u_{x3}$$

$$u_y = u_{y0} + z u_{y1} + z^2 u_{y2} + z^3 u_{y3}$$

$$u_z = u_{z0} + z u_{z1} + z^2 u_{z2} \qquad\qquad (24a\text{-}c)$$

A multi-points error evaluation along the thickness proposed by Carrera et al. [30] is implemented. The error of the new models and those used for comparison on a reference solution is evaluated through the following formula:

$$e = 100 \frac{\sum_{i=1}^{N_p} \left| Q^i - Q_{ref}^i \right|}{max Q_{ref} \cdot N_p} \qquad\qquad (25)$$

where Q can be a stress/displacement component and N_p is the number of points along the thickness on which the entity Q is computed.

4.1 Aluminum plate

The material properties are E= 73 GPa and $\upsilon = 0.34$. For each thickness ratio, an LD4 model is set as the reference model. Tables 4 and 5 present the results from the LD4 model and the full expansions adopted in this paper. The results are in perfect accordance with three-dimensional exact elasticity results obtained in [56].

Figure 2 shows the BTDs of normal stress $\overline{\sigma}_{xx}$ using polynomial and non-polynomial models for three different thickness ratios (a/h = 2.5, 5 and 50). Polynomial model BTDs are in perfect agreement with the ones developed by Petrolo et al. [32]. Best models with six unknown variables are reported in Table 6, where M_E reports the ratio of active terms and the number of the full model variables. For instance, for a thickness ratio a/h = 2.5, the best *sin* model with 6 variables provide an error of 1.2872% with respect to LD4 and is based on the following displacement field:

$$u_x = z u_{x1} + \sin\left(\frac{z}{h}\right) u_{x3} + \cos^2\left(\frac{z}{h}\right) u_{x4}$$

$$u_y = \sin\left(\frac{z}{h}\right) u_{y3} \tag{26a-c}$$

$$u_z = u_{z0} + \sin\left(\frac{z}{h}\right) u_{z3}$$

The best models of Table 6 are used to plot the normal $\overline{\sigma}_{xx}$ distribution along thickness in Fig. 3, and comparisons of the accuracy of the best models for a given number active terms with classical and higher order models can be found in Table 7.

The results suggest that:

- For thick and moderately thick plates, the use of best models based on *sin* expansions to compute $\overline{\sigma}_{xx}$ is convenient. In fact, error levels of about 1% can be obtained with less unknown variables.
- For thin plates, all best models are practically equivalent.
- The reduced models can reproduce the through-the-thickness stress distribution accurately.

- <mark>Theories included in the BTD presents better accuracies than the classical and higher order theories.</mark>

4.2 Bimetallic Plate

A bimetallic square plate used in [31] is considered as a second study case. Two layers with the same thickness are considered. The material properties are Titanium (E = 110 GPa, v = 0.34) for the top plate and Aluminum (E = 70.3 GPa, v = 0.33) for the bottom plate. Tables 8 and 9 show the reference LD4 solutions for axial and shear stress, respectively. The results of full non-polynomial expansions are reported too. Thick plates are considered. Figure 4 shows BTDs for $\overline{\sigma}_{xx}$, whereas Fig. 5 shows the through the thickness distributions provided by those models in Table 10. Similarly, Figs. 6 and 7 show the results related to $\overline{\sigma}_{xz}$.

The results suggest that

- As for the one-layer case, the BTD based on *sin* offers less cumbersome models than the others.
- As for $\overline{\sigma}_{xx}$, the through-the-thickness distribution of $\overline{\sigma}_{xz}$ can be accurately detected by the reduced models.
- A given reduced model can give fairly different errors as soon as different outputs are considered. This confirms the strong problem dependency nature of refined structural models.

4.2 Functionally Graded Plate

A functionally graded square plate considered in Ref. [18] is used as a final study case. The plate is graded across the thickness from Alumina (E = 380 GPa, v = 0.3) on the top to Aluminum (E = 70 GPa, v = 0.3) on the bottom. Table 11 reports the models assement with the reference solution presented in Ref. [18]. BTD results are computed for two different thickness ratios (a/h = 2.5 and 5) with various exponents p = 1, 4 and 10. Figures 8-10 presents the BTDs for normal stress $\overline{\sigma}_{xx}$ and shear stress $\overline{\sigma}_{xz}$ for each exponent p. In Table 12, 6 reduced models are presented with their respective through the thickness stress distributions found in figure 11 and 12 for $\overline{\sigma}_{xx}$ and $\overline{\sigma}_{xz}$ respectively. The results reported for the functional graduated plate suggest that:

- Reduced models derived from non-polynomial expansions can reproduce the through thickness stress distribution from FGP accurately.
- For higher exponents *p* reduced models require less terms to obtain results closer to the reference solution. By considering an exponent p=10, for very thick plates, models based on the *hyp* expansion can compute the $\overline{\sigma}_{xx}$ stress with an error of 0.43%, and in the thick plates case an error of only 0.21% can be achieved by using only 5 unknown variables.
- All around the BTDs suggest the *sin* model offer better reduced models to evaluate $\overline{\sigma}_{xx}$ and $\overline{\sigma}_{xz}$ stresses, while the *hyp* model is particularly good evaluating the $\overline{\sigma}_{xx}$ stress of functionally graded plates of high exponents *p*.

5. Conclusions

The effectiveness of non-polynomial terms on plate theories have been investigated in this paper. The axiomatic/asymptotic method (AAM) has been employed to build reduced models for metallic, bimetallic and functionally graded plates. Accuracies of equivalent single layer reduced models have been compared to layer-wise full models whose values are in excellent agreement with 3D results. Thick and thin simply-supported plates have been analyzed using the Carrera Unified Formulation (CUF) and the Navier-type closed form solution. Best Theory Diagrams (BTDs) have been obtained to provide guidelines for the development of refined plate models based on non-polynomial expansions.

The following main conclusions can be drawn:

- In the case of thin plates, all the considered expansion models provide fairly similar results.
- On the other hand, for thick plates, the *sin* model proved to be the best option.
- It has been confirmed that the development of the refined model is strongly problem dependent. In particular, a set of variables can provide significantly different accuracies as soon as different output variables are considered.
- The combined use of CUF and AAM can represent a contribution to the systematic construction of refined models to be used as reference solutions to compare any

other theory. In particular, the BTD can be seen as a tool to benchmark future developments in this field.

References

[1] Kirchhoff G. Über das Gleichgewicht und die Bewegung einer elastishen Scheibe. J Angew Math 1850; 40, pp. 51-88.

[2] Love A. The Mathematical theory of elasticity. Cambridge University Press, Cambridge, 1927.

[3] Reissner E. The effect of transverse shear deformation on the bending of elastic plates. J Appl Mech 1945; 12, pp.69-76.

[4] Mindlin RD. Influence of rotatory inertia and shear in flexural motion of isotropic elastic plates. J Appl Mech 1951; 18, pp 1031-1036.

[5] Reddy JN. A simple higher-order theory for laminated composite plates. J Appl Mech 1984; 51(4), pp. 745-752.

[6] Reddy JN. Analysis of functionally graded plates, Int. J. Numer. Methods Eng 2000. 47, pp. 663–684.

[7] Reddy JN. A general non-linear third-order theory of plates with moderate thickness. Int. J. Non-Linear Mechanics 1990, 25(6), pp. 677-689.

[8] Carrera E. A class of two-dimensional theories for multilayered plates analysis. Atti Accademia delle Scienze di Torino, Atti della Accademia delle Scienze di Torino, Classe di Scienze Fisiche, Matematiche e Naturali 1995, 19-20, pp. 49-87

[9] Carrera E. Theories and finite elements for multilayered plates and shells: a unified compact formulation with numerical assessment and benchmarking. Archives of Computational Methods in Engineering 2003; 10(3), 215–297.

[10] Carrera E, Giunta G, Petrolo M. Beam structures, classical and advanced theories, New Delhi: Wiley; 2011.

[11] Carrera E, Cinefra M, Petrolo M, Zappino E. Finite Element Analysis of Structures through Unified Formulation, New Delhi: Wiley; 2014.

[12] Brischetto S, Leetsch R, Carrera E, Wallmersperger T, Kröplin B. Thermo-Mechanical Bending of Functionally Graded Plates, Journal of Thermal Stresses 2008, 31, pp. 286-308

[13] Brischetto S, Carrera E. Advanced mixed theories for bending analysis of functionally graded plates, Computers and Structures 2008, 88, pp. 1474-1483

[14] Carrera E, Brischetto S, Robaldo A. Variable Kinematic Model for the Analysis of Functionally Graded Material Plates, AIAA Journal 2008, 46 (1), pp. 194-203

[15] Brischetto S, Carrera E. Refined 2D Models for the Analysis of Functionally Graded Piezoelectric Plates, Journal of Intelligent Material Systems and Structures 2009, 20, pp. 1783-1797

[16] Carrera E, Brischetto S, Cinefra M, Soave M. Refined and Advanced Models for Multilayered Plates and Shells Embedding Functionally Graded Material Layers, Mechanics of Advanced Materials and Structures 2010, 17, pp. 603-621

[17] Brischetto S, Carrera E. Advanced mixed theories for bending analysis of functionally graded plates, Computers and Structures 2010, 88, pp. 1474-1483

[18] Carrera E, Brischetto S, Cinefra M, Soave M. Effects of thickness stretching in functionally graded plates and shells, Composites: Part B 2011, 42, pp. 123-133

[19] Carrera E, Petrolo M. Guidelines and recommendation to construct theories for metallic and composite plates. AIAA Journal 2010, 48(12), pp. 2852–2866.

[20] Carrera E, Petrolo M. On the effectiveness of higher-order terms in refined beam theories. Journal of Applied Mechanics 2011, 78(2), pp. 1–17.

[21] Carrera E, Miglioretti F, Petrolo M. Guidelines and recommendations on the use of higher order finite elements for bending analysis of plates, Int J Comput Methods Eng Sci Mech 2011; 12(6), pp. 303-324.

[22] Carrera E, Miglioretti F, Petrolo M. Accuracy of refined finite elements for laminated plate analysis. Composite Structures 2011, 93(5), pp. 1311-1327.

[23] Carrera E, Miglioretti F, Petrolo M. Computations and evaluations of higher-order theories for free vibration analysis of beams. Journal of Sound and Vibration 2012; 331:4269-4284. doi: 10.1016/j.jsv.2012.04.017.

[24] Carrera E, Miglioretti F. Selection of appropriate multilayered plate theories by using a genetic like algorithm. Composite Structures 2012, 94(3), pp. 1175-1186.

[25] Mashat DS, Carrera E, Zenkour AM, Khateeb Al. Use of axiomatic/asymptotic approach to evaluate various refined theories for sandwich shells. Composite Structures 2013; 109, pp. 139-149.

[26] Mashat DS, Carrera E, Zenkour AM, Khateeb Al. Axiomatic/asymptotic evaluation of multilayered plate theories by using single and multi-points error criteria. Composite Structures 2013; 106, pp. 393-406.

[27] Mashat DS, Carrera E, Zenkour AM, Al Katheeb SA, Lamberti A. Evaluation of refined theories for multilayered shells via Axiomatic/Asymptotic Method, Journal of Mechanical Science and Technology 2014, 28(11), pp. 4663-4672.

[28] Cinefra M, Lamberti A, Zenkour AM, Carrera E. Axiomatic/asymptotic technique applied to refined theories for piezoelectric plates. Mechanics of Advanced materials and structures 2015, 22(1-2), pp.107-124.

[29] Carrera E, Cinefra M, Lamberti A, Zenkour AM. Axiomatic/Asymptotic Evaluation of Refined Plate Models for Thermomechanical Analysis. Journal of Thermal Stresses 2015, 38(2), pp. 165-187.

[30] Carrera E, Cinefra M, Lamberti A, Petrolo M. Results on best theories for metallic and laminated shells including layer-wise models. Composite Structures 2015, 126, pp.285-298.

[31] Petrolo M, Cinefra M, Lamberti A, Carrera E. Evaluation of mixed theories for laminated plates through the axiomatic/asymptotic method. Composites Part B: Engineering, 2015, 76, pp. 260-272.

[32] Petrolo M, Lamberti A. Axiomatic/asymptotic analysis of refined layer-wise theories for composite and sandwich plates. Mechanics of Advanced materials and structures 2016; 23(1), pp. 28-42.

[33] Petrolo M, Lamberti A, Miglioretti F. Best Theory diagram for metallic and laminated composite plates, Mechanics of Advance Materials and Structures 2016, 23(9), pp. 1114-1130.

[34] Cinefra M, Carrera E, Lamberti A, Petrolo M. Best Theory Diagrams for multilayered plates considering multifield analysis. Journal of Intelligent Material Systems and Structures In Press.

[35] Levy M. Memoire sur la theorie des plaques elastiques planes. Journal des Mathematiques Pures et Appliquees 1877; 30, pp. 219-306.

[36] Stein M. Nonlinear theory for plates and shells including the effects of transverse shearing. AIAA Journal 1986; 24(9), pp. 1537-1544.

[37] Touratier M. An efficient standard plate theory, Int. J. Eng. Sci. 1991; 29(8), pp. 901–916.

[38] Karama M, Afaq KS, Mistou S. Mechanical behavior of laminated composite beam by the new multi-layered laminated composite structures model with transverse shear stress continuity. Int. J. Solids Struct 2003; 40(6), pp. 1525–1546

[39] Shimpi RP, Ghugal YM. A new layerwise trigonometric shear deformation theory for twolayered cross-ply beams. Composite Science and Technology 2001, 61(9), pp. 1271–1283.

[40] Arya H, Shimpi RP, Naik NK. A zigzag model for laminated composite beams. Composite Structures 2002; 56(1), pp. 21–24.

[41] Ferreira AJ., Roque C., Jorge RM. Analysis of composite plates by trigonometric shear deformation theory and multiquadrics. Computers and Structures 2005; 83(27), pp. 2225–2237.

[42] Neves AM, Ferreira AJ, Carrera E, Cinefra M, Jorge RM, Soares CM. Buckling analysis of sandwich plates with functionally graded skins using a new quasi-3D hyperbolic sine shear deformation theory and collocation with radial basis functions. Zeitschrift für Angewandte Mathematik und Mechanik 2012; 92(9), pp. 749-766.

[43] Neves AM, Ferreira AJ, Carrera E, Cinefra M, Roque CM, Jorge RM, Soares CM. A quasi-3D hyperbolic shear deformation theory for the static and free vibration analysis of functionally graded plates. Composite Structures 2012; 94, pp. 1814-1825

[44] Neves AM, Ferreira AJ, Carrera E, Roque CM, Cinefra M, Jorge RM, Soares CM. A quasi-3D sinusoidal shear deformation theory for the static and free vibration analysis of functionally graded plates. Composites: Part B 2012; 43, pp. 711-725

[45] Neves AM, Ferreira AJ, Carrera E, Cinefra M, Jorge RM, Soares CM. Static analysis of functionally graded sandwich plates according to a hyperbolic theory considering Zig-Zag and warping effects. Advances in Engineering Software 2012; 52, pp. 30-43

[46] Mantari JL, Oktem AS, Soares CG. A new trigonometric shear deformation theory for isotropic, laminated composite and sandwich plates. International Journal of Solids and Structures 2012; 49(1), pp. 43-53.

[47] Tounsi A, Ahmed MS, Benyoucef S, Adda EA. A refined trigonometric shear deformation theory for thermoelastic bending of functionally graded sanwich plates. Aerospace Science and Technology 2013; 24, pp 209-220.

[48] Sahoo R, Singh BN. A new trigonometric zigzag theory for static analysis of laminated composite and sanwich plates. Aerospace Science and Technology 2014; 35, pp. 15-28.

[49] Mantari JL, Ramos IA, Carrera E, Petrolo M. Static analysis of functionally graded plates using new non-polynomial displacement fields via Carrera Unified Formulation. Composites Part B: Engineering 2016; 89, pp. 127-142.

[50] Ramos IA, Mantari JL, Zenkour AM, Laminated composite plates subject to thermal load using trigonometrical theory based on Carrera Unified Formulation. Composite Structures 2016; 143, pp 324-335.

[51] Filippi M, Carrera E, Zenkour AM. Static analyses of FGM beams by various theories and finite elements. Composites Part B: Engineering 2015; 72, pp. 1-9.

[52] Filippi M, Petrolo M, Valvano S, Carrera E. Analysis of laminated composites and sandwich structures by trigonometric, exponential and miscellaneous polynomials and a MITC9 plate element. Composite Structures 2016; 150, pp. 103-114.

[53] Mantari JL. General recommendations to develp 4-unknows quasi-3D HSDTs to study FGMs. Aerospace Science and Technology 2016; 58, pp. 559-570.

[54] Mantari JL. Computational development of a 4 unknowns trigonometric quasi - 3D shear deformation theory to study advanced sandwich plates and shells. International Journal of Applied Mechanics 2016; 8(4).

[55] Mantari JL. A simple polynomial quasi - 3D HSDT with four unknowns to study FGPs. Reddy´s HSDT assessment. Composite Structures 2016; 137, pp. 114-120.

[56] Carrera E, Giunta G, Brischetto S. Hierarchical closed form solutions for plates bent by localized transverse loadings. Journal of Zhejiang University - Science A: Applied Physics & Engineering 2007, 8(7), pp. 1026–1037.

[57] Pandya B, Kant T. Finite Element Analysis of Laminated Composite Plates Using High-Order Displacement Model. Composites Science and Technology 1988, 32(2), pp. 137–155.

[58] Roque C, Ferreira A, Jorge R. A radial basis function approach for the free vibration analysis of functionally graded plates using a refined theory. Journal of Sound and Vibration 2007, 300, pp. 1048–1070.

[59] Kant T, Manjunatha B. An Unsymmetric Frc Laminate c° Finite Element Model With 12 degrees of Freedom Per Node. Eng Comput 1988, 5(4), pp. 292–308.

[60] Lo K, Christensen R, Wu E. A High-Order Theory of Plate Deformation—Part 2: Laminated Plates. J. Appl. Mech 1977, 44(4), pp. 669–676.

[61] Zenkour AM. A simple four-unknown refined theory for bending analysis of functionally graded plates. Applied Mathematical Modelling 2013, 37(20-21), pp. 9041–9051.

[62] Zenkour AM. Bending analysis of functionally graded sandwich plates using a simple four-unknown shear and normal deformations theory. Journal of Sandwich Structures & Materials 2013, 15(6), pp. 629–656.

[63] Zenkour AM. Bending of FGM plates by a simplified four-unknown shear and normal deformations theory. International Journal of Applied Mechanics 2013, 5(2) 1350020 (15 pages).

[64] Thai C, Zenkour AM, Abdel M, Thai N. A simple four-unknown shear and normal deformations theory for functionally graded isotropic and sandwich plates based on isogeometric analysis, Composite Structures 2016, 139, pp. 77–95.

Tables caption

Table 1: Expansion terms of the proposed theories.

Table 2: Example of model representation.

Table 3: Symbols to indicate the status of a displacement variable.

Table 4: LD4 model assessment for the Aluminum plate, top $\bar{\sigma}_{xx}$ values.

Table 5: Model assessment of the proposed theories for the Aluminum plate, top, and bottom $\bar{\sigma}_{xx}$ values.

Table 6: Best reduced models with six unknown variables for $\bar{\sigma}_{xx}$, aluminum plate.

Table 7: Comparison between best reduced models and classical and higher order theories.

Table 8: Model assessments of the proposed theories for the bimetallic plate, top, and bottom $\bar{\sigma}_{xx}$ values.

Table 9: Model assessments of the proposed theories for the bimetallic plate, $z = 0$ $\bar{\sigma}_{xz}$ values.

Table 10: Reduced models with six unknown variables for $\bar{\sigma}_{xx}$ and $\bar{\sigma}_{xz}$, bimetallic plate.

Table 11. Model assessments of the proposed theories for the functionally graded plate, $\bar{\sigma}_{xx}$ $(h/3)$ and $\bar{w}(0)$ values.

Table 12. Reduced models with six unknown variables for $\bar{\sigma}_{xx}$ and $\bar{\sigma}_{xz}$, functionally graded plate.

Figures Caption

Figure 1. Plate reference system and notations.

Figure 2. Comparison between BTDs of polynomial and non-polynomial models for $\bar{\sigma}_{xx}$ stress, aluminium plate, (a) $a/h = 2.5$, (b) $a/h = 5$, (c) $a/h = 50$.

Figure 3. $\bar{\sigma}_{xx}$ distribution along the thickness for the reduced models of Table 6, (a) $a/h = 2.5$, (b) $a/h = 5$, (c) $a/h = 50$.

Figure 4. Comparison between BTDs of polynomial and non-polynomial models for $\bar{\sigma}_{xx}$, bimetallic plate, (a) $a/h = 2.5$, (b) $a/h = 5$.

Figure 5. $\bar{\sigma}_{xx}$ stress distribution along the thickness for the reduced models from Table 9, (a) $a/h = 2.5$, (b) $a/h = 5$.

Figure 6. Comparison between BTDs of polynomial and non-polynomial models or $\bar{\sigma}_{xz}$, bimetallic plate, (a) $a/h = 2.5$, (b) $a/h = 5$.

Figure 7. $\bar{\sigma}_{xz}$ stress distribution along the thickness for the reduced models from Table 9, (a) $a/h = 2.5$, (b) $a/h = 5$.

Figure 8. Comparison between BTDs of polynomial and non-polynomial models for $p = 1$, functionally graded plate, (a) $a/h = 2.5$ $\bar{\sigma}_{xx}$, (b) $a/h = 5$ $\bar{\sigma}_{xx}$, (c) $a/h = 2.5$ $\bar{\sigma}_{xz}$, (d) $a/h = 5$ $\bar{\sigma}_{xz}$,

Figure 9. Comparison between BTDs of polynomial and non-polynomial models for $p = 4$, functionally graded plate, (a) $a/h = 2.5$ $\bar{\sigma}_{xx}$, (b) $a/h = 5$ $\bar{\sigma}_{xx}$, (c) $a/h = 2.5$ $\bar{\sigma}_{xz}$, (d) $a/h = 5$ $\bar{\sigma}_{xz}$,

Figure 10. Comparison between BTDs of polynomial and non-polynomial models for $p = 10$ functionally graded plate, (a) $a/h = 2.5$ $\bar{\sigma}_{xx}$, (b) $a/h = 5$ $\bar{\sigma}_{xx}$, (c) $a/h = 2.5$ $\bar{\sigma}_{xz}$, (d) $a/h = 5$ $\bar{\sigma}_{xz}$,

Figure 11. $\bar{\sigma}_{xx}$ stress distribution along the thickness for the reduced models from Table 11, (a) $a/h = 2.5$, (b) $a/h = 5$.

Figure 12. $\bar{\sigma}_{xz}$ stress distribution along the thickness for the reduced models from Table 11, (a) $a/h = 2.5$, (b) $a/h = 5$.

Tables

Table 1.

Model	F_0	F_1	F_2	F_3	F_4
pol	1	z	z^2	z^3	z^4
sin	1	z	$\cos\left(\frac{z}{h}\right)$	$\sin\left(\frac{z}{h}\right)$	$\cos^2\left(\frac{z}{h}\right)$
hyp	1	z	$\cosh\left(\frac{z}{h}\right)$	$\sinh\left(\frac{z}{h}\right)$	$\cosh^2\left(\frac{z}{h}\right)$
exp	1	z	$e^{\frac{z}{h}}$	$e^{\frac{2z}{h}}$	$e^{\frac{3z}{h}}$

Table 2.

Full model representation						Reduced model representation				
▲	▲	▲	▲	▲		▲	Δ	▲	▲	▲
▲	▲	▲	▲	▲		▲	▲	▲	▲	▲
▲	▲	▲	▲	▲		▲	▲	▲	▲	▲

Table 3.

Active term	Inactive terms
▲	Δ

Table 4.

a/h	100	10	5	2
Ref [56]	0.2037	0.2068	0.2168	0.3145
LD4	0.2037	0.2068	0.2169	0.3165

Table 5

a/h	50		5		2.5	
LD4	0.2038	-0.2037	0.2169	-0.2083	0.2681	-0.2145
pol	0.2038	-0.2037	0.2169	-0.2083	0.2681	-0.2145
sin	0.2038	-0.2037	0.2170	-0.2084	0.2685	-0.2148
hyp	0.2038	-0.2037	0.2168	-0.2083	0.2677	-0.2142
exp	0.2030	-0.2045	0.2140	-0.2112	0.2590	-0.2230

Table 6.

	pol	sin	hyp	exp	M_E
		a/h = 2.5			
Error	2.2678 %	1.2878 %	1.8582 %	2.5562 %	6/15
		a/h = 5			
Error	0.6438 %	0.4244 %	0.3853 %	1.0722 %	6/15
		a/h = 50			
Error	0.0062 %	0.0062 %	0.0062 %	0.0115 %	6/15

Table 7

		a/h = 2.5			
M_E = 12/15	pol	sin	hyp	exp	Kant [59]
Error $\bar{\sigma}_{xx}$	0.2080 %	0.0834 %	0.2079 %	0.6562 %	3.0414 %
M_E = 11/15	pol	sin	hyp	exp	Lo [60]
Error $\bar{\sigma}_{xx}$	0.2138 %	0.2032 %	0.2079 %	0.7182 %	3.1021 %

$M_E = 9/15$	pol	sin	hyp	exp	Pandya [57]
Error $\bar{\sigma}_{xx}$	1.2159 %	0.7619 %	0.4902 %	0.9292 %	5.7696 %
$M_E = 7/15$	pol	sin	hyp	exp	Roque [58]
Error $\bar{\sigma}_{xx}$	1.8438 %	1.1637 %	1.3231 %	1.8023 %	5.7696 %
$M_E = 5/15$	pol	sin	hyp	exp	FSDT
Error $\bar{\sigma}_{xx}$	3.0489 %	3.5226 %	2.825 %	3.1384 %	5.7202 %
			$a/h = 5$		
$M_E = 12/15$	pol	sin	hyp	exp	Kant [59]
Error $\bar{\sigma}_{xx}$	0.0166 %	0.0174 %	0.0176 %	0.2248 %	0.9863 %
$M_E = 11/15$	pol	sin	hyp	exp	Lo [60]
Error $\bar{\sigma}_{xx}$	0.0166 %	0.0221 %	0.0176 %	0.2248 %	0.9928 %
$M_E = 9/15$	pol	sin	hyp	exp	Pandya [57]
Error $\bar{\sigma}_{xx}$	0.3436 %	0.3115 %	0.0689 %	0.2323 %	1.6057 %
$M_E = 7/15$	pol	sin	hyp	exp	Roque [58]
Error $\bar{\sigma}_{xx}$	0.5067 %	0.3245 %	0.3511 %	0.4834 %	1.6057 %
$M_E = 5/15$	pol	sin	hyp	exp	FSDT
Error $\bar{\sigma}_{xx}$	1.1126 %	1.1042 %	0.5579 %	1.0556 %	1.9422 %
			$a/h = 50$		
$M_E = 12/15$	pol	Sin	hyp	exp	Kant [59]
Error $\bar{\sigma}_{xx}$	0.0000 %	0.0051 %	0.0046 %	0.0081 %	0.0107 %
$M_E = 11/15$	pol	Sin	hyp	exp	Lo [60]
Error $\bar{\sigma}_{xx}$	0.0000 %	0.0051 %	0.0046 %	0.0081 %	0.0107 %
$M_E = 9/15$	pol	sin	hyp	exp	Pandya [57]
Error $\bar{\sigma}_{xx}$	0.0038 %	0.0052 %	0.0049 %	0.0081 %	0.0169 %
$M_E = 7/15$	pol	sin	hyp	exp	Roque [58]
Error $\bar{\sigma}_{xx}$	0.0048 %	0.0062 %	0.0062 %	0.0081 %	0.0169 %
$M_E = 5/15$	pol	sin	hyp	exp	FSDT
Error $\bar{\sigma}_{xx}$	0.0115 %	0.0115 %	0.0115 %	0.0115 %	0.0211 %

Table 8

a/h	5		2.5	
LD4	0.2482	-0.1830	0.3114	-0.1834
pol	0.2472	-0.1845	0.3100	-0.1877
sin	0.2474	-0.1846	0.3104	-0.1878
hyp	0.2472	-0.1845	0.3096	-0.1876
exp	0.2453	-0.1855	0.3040	-0.1894

Table 9.

a/h	5	2.5
LD4	0.2328	0.2241

pol	0.2332	0.2255
sin	0.2332	0.2255
hyp	0.2332	0.2255
exp	0.2329	0.2247

Table 10.

	pol	sin	hyp	exp	M_E

a/h = 5
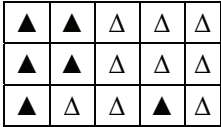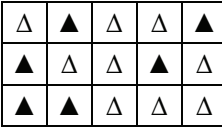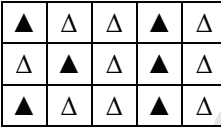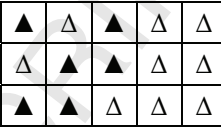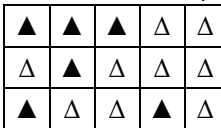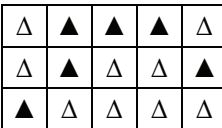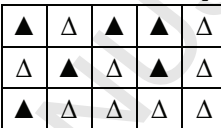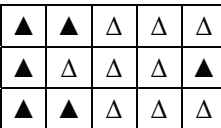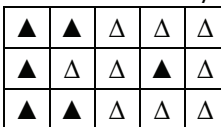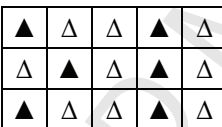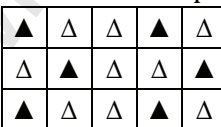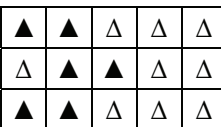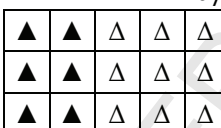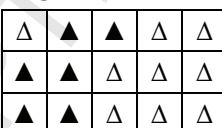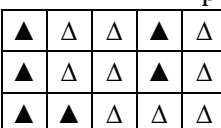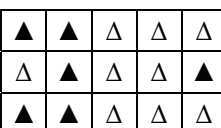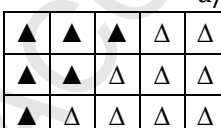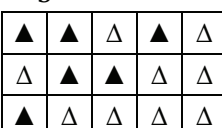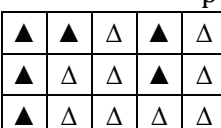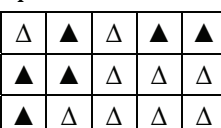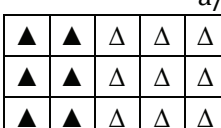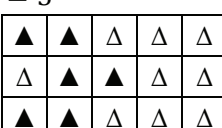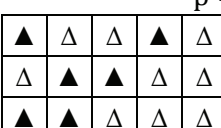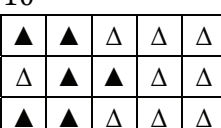
pol	sin	hyp	exp	M_E
▲ ▲ △ ▲ △	△ ▲ ▲ △ △	▲ △ △ ▲ △	▲ ▲ △ △ ▲	
▲ ▲ △ △ △	△ ▲ ▲ △ △	▲ △ △ ▲ △	▲ ▲ △ △ △	6/15
▲ △ △ △ △	▲ ▲ △ △ △	▲ ▲ △ △ △	▲ △ △ △ △	

Error		pol	sin	hyp	exp
	σ_{xx}	1.4817 %	1.3002 %	0.9462 %	1.5786 %
	σ_{xz}	0.6337 %	0.4272 %	0.9180 %	0.4731 %

a/h = 2.5

pol	sin	hyp	exp	M_E
▲ ▲ ▲ △ △	△ △ △ ▲ ▲	▲ △ ▲ ▲ △	△ ▲ ▲ △ ▲	
△ ▲ △ △ △	△ ▲ △ ▲ △	△ △ △ ▲ △	△ ▲ △ △ △	6/15
▲ ▲ △ △ △	▲ ▲ △ △ △	△ △ ▲ ▲ △	▲ ▲ △ △ △	

Error		pol	sin	hyp	exp
	σ_{xx}	3.4770 %	2.6924 %	3.2039 %	2.3041 %
	σ_{xz}	2.1055 %	1.4365 %	1.8642 %	1.3696 %

Table 11

p	Theory	$\overline{\sigma}_{xx_{h/3}}$			$\overline{w}(0)$		
		a/h=4	a/h=10	a/h=100	a/h=4	a/h=10	a/h=100
1	Ref. [18]	0.6221	1.5064	14.9692	0.7171	0.5875	0.5625
1	LD4	0.6221	1.5064	14.9692	0.7171	0.5875	0.5625
1	Pol	0.6221	1.5064	14.9692	0.7171	0.5875	0.5625
1	Sin	0.6218	1.5062	14.9682	0.7171	0.5875	0.5625
1	Hyp	0.6223	1.5064	14.9683	0.7171	0.5875	0.5625
1	Exp	0.6243	1.5090	14.9899	0.7171	0.5875	0.5625
4	Ref. [18]	0.4877	1.1971	11.9227	1.1585	0.8822	0.8287
4	LD4	0.4877	1.1971	11.9227	1.1585	0.8822	0.8287
4	Pol	0.4877	1.1971	11.9227	1.1585	0.8822	0.8287
4	Sin	0.4874	1.1969	11.9219	1.1585	0.8822	0.8287
4	Hyp	0.4880	1.1972	11.9220	1.1585	0.8822	0.8287
4	Exp	0.4858	1.1976	11.9389	1.1587	0.8822	0.8287
10	Ref. [18]	0.3696	0.8966	8.9078	1.3745	1.0072	0.9362
10	LD4	0.3696	0.8966	8.9078	1.3745	1.0072	0.9362
10	Pol	0.3696	0.8966	8.9078	1.3745	1.0072	0.9362
10	Sin	0.3690	0.8963	8.9073	1.3746	1.0072	0.9362

10	Hyp	0.3700	0.8967	8.9074	1.3745	1.0072	0.9362
10	Exp	0.3740	0.8994	8.9194	1.3756	1.0073	0.9362

Table 12.

	pol	sin	hyp	exp	M_E

a/h = 2.5, p = 1

pol:
```
▲ ▲ Δ Δ Δ
▲ ▲ Δ Δ Δ
▲ Δ Δ ▲ Δ
```
sin:
```
Δ ▲ Δ Δ ▲
▲ Δ Δ ▲ Δ
▲ ▲ Δ Δ Δ
```
hyp:
```
▲ Δ Δ ▲ Δ
Δ ▲ Δ ▲ Δ
▲ Δ Δ ▲ Δ
```
exp:
```
▲ Δ ▲ Δ Δ
Δ ▲ ▲ Δ Δ
▲ ▲ Δ Δ Δ
```
$M_E = 6/15$

Error	pol	sin	hyp	exp
σ_{xx}	2.5763 %	2.2435 %	2.4130 %	1.8174 %
σ_{xz}	1.5310 %	1.4183 %	1.7918 %	1.0223 %

a/h = 2.5, p = 4

pol:
```
▲ ▲ ▲ Δ Δ
Δ ▲ Δ Δ Δ
▲ Δ Δ ▲ Δ
```
sin:
```
Δ ▲ ▲ ▲ Δ
Δ ▲ Δ Δ ▲
▲ Δ Δ Δ Δ
```
hyp:
```
▲ Δ ▲ ▲ Δ
Δ ▲ Δ ▲ Δ
▲ Δ Δ Δ Δ
```
exp:
```
▲ ▲ Δ Δ Δ
▲ Δ Δ Δ ▲
▲ ▲ Δ Δ Δ
```
$M_E = 6/15$

Error	pol	sin	hyp	exp
σ_{xx}	2.8118 %	2.0406 %	2.8017 %	1.8488 %
σ_{xz}	1.0690 %	1.3068 %	0.9622 %	1.8022 %

a/h = 2.5, p = 10

pol:
```
▲ ▲ Δ Δ Δ
▲ Δ Δ ▲ Δ
▲ ▲ Δ Δ Δ
```
sin:
```
▲ Δ Δ ▲ Δ
Δ ▲ Δ ▲ Δ
▲ Δ Δ ▲ Δ
```
hyp:
```
▲ Δ Δ ▲ Δ
Δ ▲ Δ Δ ▲
▲ Δ Δ ▲ Δ
```
exp:
```
▲ ▲ Δ Δ Δ
Δ ▲ ▲ Δ Δ
▲ ▲ Δ Δ Δ
```
$M_E = 6/15$

Error	pol	sin	hyp	exp
σ_{xx}	1.9334 %	1.7682 %	1.4593 %	1.4713 %
σ_{xz}	0.7909 %	0.8724 %	1.7993 %	1.8669 %

a/h = 5, p = 1

pol:
```
▲ ▲ Δ Δ Δ
▲ ▲ Δ Δ Δ
▲ ▲ Δ Δ Δ
```
sin:
```
Δ ▲ ▲ Δ Δ
▲ ▲ Δ Δ Δ
▲ ▲ Δ Δ Δ
```
hyp:
```
▲ Δ Δ ▲ Δ
Δ Δ Δ ▲ Δ
▲ ▲ Δ Δ Δ
```
exp:
```
▲ ▲ Δ Δ Δ
Δ ▲ Δ Δ ▲
▲ ▲ Δ Δ Δ
```
$M_E = 6/15$

Error	pol	sin	hyp	exp
σ_{xx}	0.7295 %	0.5033 %	0.3731 %	0.8857 %
σ_{xz}	0.5458 %	0.3126 %	0.5419 %	0.4511 %

a/h = 5, p = 4

pol:
```
▲ ▲ ▲ Δ Δ
▲ ▲ Δ Δ Δ
▲ Δ Δ Δ Δ
```
sin:
```
▲ ▲ Δ ▲ Δ
Δ ▲ ▲ Δ Δ
▲ Δ Δ Δ Δ
```
hyp:
```
▲ ▲ Δ ▲ Δ
▲ Δ Δ ▲ Δ
▲ Δ Δ Δ Δ
```
exp:
```
Δ ▲ Δ ▲ ▲
▲ ▲ Δ Δ Δ
▲ Δ Δ Δ Δ
```
$M_E = 6/15$

Error	pol	sin	hyp	exp
σ_{xx}	0.9292 %	0.6625 %	0.6362 %	0.9681 %
σ_{xz}	0.4997 %	0.4722 %	0.4516 %	0.3857 %

a/h = 5, p = 10

pol:
```
▲ ▲ Δ Δ Δ
▲ ▲ Δ Δ Δ
▲ ▲ Δ Δ Δ
```
sin:
```
▲ ▲ Δ Δ Δ
Δ ▲ ▲ Δ Δ
▲ ▲ Δ Δ Δ
```
hyp:
```
▲ Δ Δ ▲ Δ
Δ ▲ ▲ Δ Δ
▲ Δ Δ Δ Δ
```
exp:
```
▲ ▲ Δ Δ Δ
Δ ▲ ▲ Δ Δ
▲ ▲ Δ Δ Δ
```
$M_E = 6/15$

Error	pol	sin	hyp	exp
σ_{xx}	0.3644 %	0.3932 %	0.5311 %	0.7287 %
σ_{xz}	0.4371 %	0.5455 %	0.2689 %	0.5834 %

Figures

Figure 1

Figure 2.

(a) $a/h = 2.5$

(b) $a/h = 5$

(c) $a/h = 50$

Figure 3.

(a) $a/h = 2.5$

(b) $a/h = 5$

(c) $a/h = 50$

Figure 4.

(a) $a/h = 2.5$

(b) $a/h = 5$

Figure 5.

(a) $a/h = 2.5$

(b) $a/h = 5$

Figure 6.

(a) $a/h = 2.5$

(b) $a/h = 5$

Figure 7.

(a) $a/h = 2.5$

(b) $a/h = 5$

Figure 8.

(a) $a/h = 2.5$

(b) $a/h = 5$

(c) $a/h = 2.5$

(d) $^a/_h = 5$

Figure 9

(a) $^a/_h = 2.5$

(b) $^a/_h = 5$

(c) $^a/_h = 2.5$

(d) $a/h = 5$

Figure 10

(a) $a/h = 2.5$

(b) $a/h = 5$

(c) $a/h = 2.5$

(d) $a/h = 5$

Figure 11.

(a) $a/h = 2.5$

(b) $a/h = 5$

Figure 12.

(a) $a/h = 2.5$

(b) $a/h = 5$